Polymer Journal, Vol. 35, No. 4, pp 372—378 (2003)

Solid-State NMR Characterization on the Molecular-Level Homogeneity in Lower Critical Solution Temparature Mixtures of Poly(α-methyl styrene) and Poly(2,6-dimethyl-*p*-phenylene oxide)

Ea Mor WOO,† I-Chi CHOU, Li Ling CHANG, and Hsien-Ming KAO*

Department of Chemical Engineering, National Cheng Kung University, Tainan, 701–01, Taiwan
**Department of Chemistry National Central University Chung-Li, 320–54, Taiwan*

(Received September 20, 2002; Accepted December 24, 2002)

ABSTRACT: The length scale of heterogeneity in blends of poly(2,6-dimethyl-*p*-phenylene oxide) (PPO) with poly(α-methyl styrene) (PαMS) was investigated using solid state ^{13}C NMR. The PPO/PαMS blend system was homogeneous at ambient, but phase separation at or above the lower critical solution temperature (LCST) was confirmed by polarized-light microscopy (PLM) and differential scanning calorimetry (DSC). Fourier-transform infrared spectroscopy (FT-IR) characterization confirmed that there was no specific interaction between PPO and PαMS. The scales of homogeneity in the blend were examined. ^1H spin-relaxation times in the laboratory frame (T_1^H) and in the rotating frame ($T_{1\rho}^H$) were measured for PPO/PαMS blends of various compositions and neat polymer components (PPO, PαMS). $T_{1\rho}^H$ data indicated that PPO and PαMS are mixed at the molecular level for all compositions, showing that the miscibility scale is comparable with that of the classical blend system of PPO and polystyrene (PS).

KEY WORDS Solid State ^{13}C NMR / Poly(α-methyl styrene) / Poly(2,6-dimethyl-*p*-phenylene oxide) / Phase Homogeneity / Lower Critical Solution Temperature (LCST) / Blend /

The lack of special functional groups in its chain structure makes polystyrene (PS) immiscible with most thermoplastic polymers, with only some notable exceptions. Blends of PS with poly(2,6-dimethyl-*p*-phenylene oxide) (PPO) have been extensively investigated by thermal analysis, FT-IR, NMR, and found to be fully miscible several decades ago.[1–9] The phase behavior of PS/poly(α-methyl styrene) (PαMS) blend systems has also been investigated.[10–16] Interestingly, although the structures of PS and PαMS differ only by a methyl group ($-CH_3$) at the α-position on the main chain, the PS/PαMS blend system is immiscible at ambient temperature but turns out to be miscible above 240 °C depending on molecular weights of their blends. This is known as upper critical solution temperature (UCST) behavior. Blends of PPO with poly(4-methyl styrene) (P4MS) were also studied.[17–19] For the PPO/PαMS blend, there have been some comparative studies. Mikes and Morawetz[20] found that the extent of miscibility of PPO/PαMS blend was lower than that of PPO/PS. In addition, Kressler *et al.*[21] reported that PαMS is miscible with PPO by using thermal analysis and FT-IR. However, more detailed and in-depth studies on the scales of the phase homogeneity in PPO and PαMS are needed.

Solid-state NMR has been utilized in analyzing miscibility, phase structure or heterogeneity in polymer mixtures on a molecular scale.[22–24] NMR is especially useful in studies on miscibility of polymer blend systems containing complex phase structures beyond the resolution limits of conventional microscopy or thermal analysis. Spin-lattice relaxation times of ^{13}C nuclei due to dipole–dipole interactions between carbons and protons in the rotating frame ($T_{1\rho}^H$) and laboratory frame (T_1^H) are sensitive to heterogeneity in blends and can be used to establish upper and lower limits of length scales of heterogeneity. Stejskal *et al.*[25] demonstrated the use of well-resolved ^{13}C NMR spectra to monitor ^1H relaxation behavior. Several studies of polymer/polymer miscibility have been reported using T_1^H, $T_{1\rho}^H$, and spin diffusion.[26–34] Since the proton spin-lattice relaxation reflects the intimate relation of the configuration of the component polymers through proton spin-diffusion processes, measurements of proton spin-lattice relaxation times for specific carbons in the blend provide information on micro-heterogeneity. The length scale of heterogeneity from a few angstroms (Å) to some tens of nanometers (nm) can be evaluated approximately from $T_{1\rho}^H$ and T_1^H for measuring compositional heterogeneity in length scales limited by spin diffusion. The main difference between T_1^H and $T_{1\rho}^H$ is in the time scale. T_1^H with a longer time scale of 100 ms to few seconds characterizes the hetero-phase domains over a larger length scale within few hundred Å, while $T_{1\rho}^H$ with a shorter time scale of few milliseconds characterizes the size of domains within a shorter length scale of *ca.* 50 Å. These parameters together provide information on het-

†To whom correspondence should be addressed (Tel: +886-6-234-4486; E-mail: emwoo@mail.ncku.edu.tw).

erogeneous phase domains over the scale differing by one order of magnitude.

PS and PαMS differ only by an alpha-methyl in the repeat unit. Blends comprising PS and PαMS may show significant difference in phase behavior. Apparently, the phase homogeneity scales of PS/PPO and PαMS/PPO may differ. The any difference may be beyond the discerning limits of DSC as both blend systems exhibit single and composition-dependent T_gs. Therefore, for such occasions, NMR is indispensable. As the blend phase behavior refers to a solid state of soft matters and not a solution state, NMR would ideally be based on solid states. Thus the present work was done to obtain further evidence for comparison of heterogeneity/homogeneity scales in neat PPO, neat PαMS, and PPO/PαMS blends, which were proven earlier to be miscible systems, by solid-state NMR using ^{1}H spin-lattice relaxation time measurements.

EXPERIMENTAL

Materials and Sample Preparation

Amorphous poly(2,6-dimethyl *p*-phenylene oxide) (PPO) with an approximate M_w = 50000 g mol^{-1} (gel permeation chromatograph, GPC), polydispersity index (PI) of about 2.5 and the glass transition temperature T_g = 207 °C was purchased from a specialty polymers supplier (Polysciences, Inc., USA). Poly(α-methyl styrene) (PαMS) with an approximate M_w = 12100 g mol^{-1} (gel permeation chromatograph, GPC), with a narrow polydispersity index (PI) of about 1.1 and T_g = 160 °C, was obtained from Scientific Polymers Product (SP^2), Inc. (USA.). Blend samples in this study were prepared by solution blending and film-casting (chloroform) at 45 °C. Cast-film samples were dried in a vacuum oven for 48 h at 80 °C and solvent was completely removed.

Apparatus

Blend T_gs were measured with a differential scanning calorimeter (PerkinElmer DSC-7) equipped with an intracooler and computer for data acquisition and analysis. All T_g measurements were made at a scan rate of 20 °C min^{-1}, and T_g was taken as the onset of transition (change of the specific heat) in the DSC thermograms. Thermal treatments such as annealing and quenching were performed inside DSC cells.

A polarized-light microscope (Nikon Optiphot-2, POL) was used for observation of the phase morphology and cloud point. Solutions of blends were spread on glass slides and dried in a temperature-controlled oven and the films were examined with an optical microscope. Same blend samples for optical examination were used for thermal analysis. Samples were placed on a microscope heating stage and heated at approximately 2 °C min^{-1} from room temperature up to 350 °C.

Fourier-transform infrared spectroscopy (FT-IR, Nicolet Magna-560) was used for investigating molecular interactions between constituents. Spectra were obtained at 4 cm^{-1} resolution and average values were obtained from at least 64 scans in the standard wavenumber range of 400–4000 cm^{-1}. Thin films for FT-IR studies were obtained by casting PPO/PαMS solutions onto potassium bromide disks at 45 °C.

^{13}C CP/MAS NMR Measurements. Solid-state ^{13}C cross-polarization (CP)/magic angle spinning (MAS) NMR experiments were performed on a Bruker AVANCE-400 spectrometer equipped with a Bruker double-tuned 7 mm probe at 100.62 MHz for ^{13}C nuclei and 400.13 MHz for ^{1}H nuclei. The Hartmann–Hahn condition for ^{1}H to ^{13}C CP experiments was determined using adamantane. ^{13}C CP/MAS NMR spectra were recorded with a CP contact time of 1 ms, a repetition time of 4 s, and a spinning speed of 6.2 kHz. The ^{13}C chemical shifts were externally referenced to tetramethylsilane (TMS).

Proton Relaxation Time Measurements. T_1^H relaxation time was indirectly measured by observing ^{13}C resonance after applying the π-τ-$\pi/2$ (inversion–recovery) pulse sequence, followed by CP. For $T_{1\rho}^H$ relaxation time measurements, the spin-locking pulse sequence was applied before CP. CP contact time was set at 1 ms and spin-locking field strength was 45 kHz. Proton decoupling field strength was 60 kHz in all experiments.

RESULTS AND DISCUSSION

Phase Behavior and Thermal Characterization

Phase morphology of PPO/PαMS mixtures was preliminarily examined using a polarized-light microscope (PLM). No domains were found, and all samples appeared optically clear at a magnification of 800. Glass transitions and thermal behavior were investigated by DSC and only one apparently single T_g in all PPO/PαMS blends was found. The width of the transition was comparably narrow for all blends. This suggests quite good miscibility between component polymers according conventional criteria of polymer miscibility. Quantitative relationship between T_g and composition may help in preliminarily understanding the phase homogeneity in the molecular scales. Figure 1 shows the dependence of T_g on composition of the PPO/PαMS blend. The composition dependence relationship exhibits a negative deviation from the additiv-

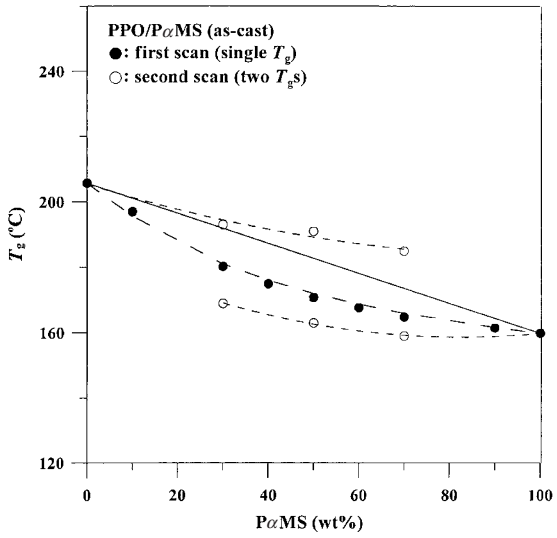

Figure 1. T_g *vs.* composition at various contents of PαMS in as-cast PPO/PαMS blends, respectively.

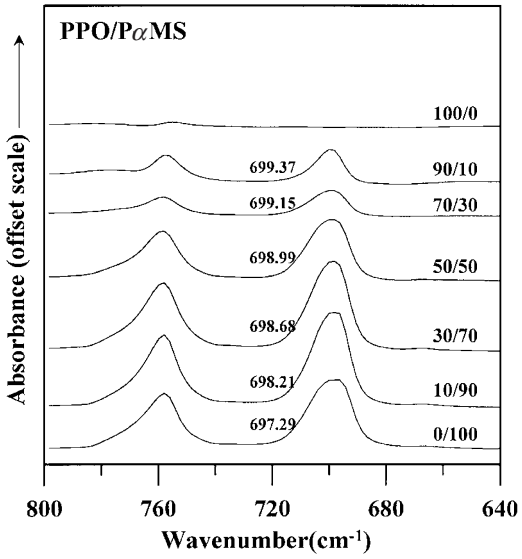

Figure 2. FT-IR spectra of aromatic C–H groups in PαMS polymer for seven different compositions of PPO/PαMS blend.

ity rule of $T_g = \omega_1 T_{g1} + k\omega_2 T_{g2}$ and also from the Fox equation of $1/T_g = \omega_1/T_g + \omega_2/T_{g2}$. We attempted to fit the T_g-composition dependence to the Gordon–Taylor equation,[35] $T_g = (\omega_1 T_{g1} + k\omega_2 T_{g2})/(\omega_1 + k\omega_2)$, where ω_i is the mass fraction of polymer component i, and k is a fitting parameter. Relatively low $k = 0.32$ was obtained, suggesting that no particularly strong specific interactions were present between PPO and PαMS in the blend, although the thermal criteria confirmed miscibility.

We looked for intermolecular interactions in PPO/PαMS blends using FT-IR. Figure 2 shows the FT-IR spectra of PPO/PαMS blends. The absorbance peak of the aromatic C–H in PαMS remained at the same frequency (*ca.* 698 cm^{-1}), and was quite independent of blend composition. No significant

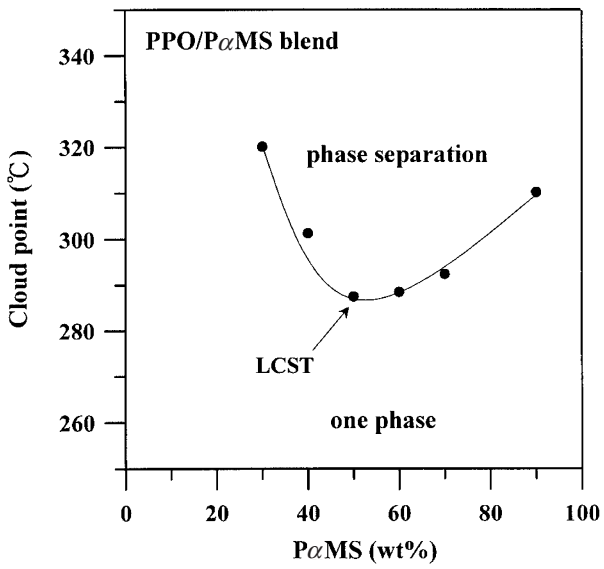

Figure 3. Plots of cloud point as a function of PαMS content in the PPO/PαMS blend.

change was observed for the ether (–O–) absorbance peak in the blend. There are thus no particularly strong specific interactions between PPO and PαMS, albeit they are miscible.

The phase morphology of the as-prepared PPO/PαMS blend was clear, homogeneous, but at certain high temperatures, the blends showed apparent heterogeneity on heating at a slow heating rate of 2°C min^{-1} to high temperatures. Figure 3 summarizes cloud point initiation temperatures for the PPO/PαMS blends of various compositions. Polarized-light microscopy showed that all blend samples changed from one phase to a phase-separated blend with a spinodal phase decomposition pattern upon heating. The lowest cloud point was usually labeled as LCST, and an LCST near 287 °C was identified for the PPO/PαMS (50/50) blend. The as-prepared blends below the cloud points were homogeneous and free of any micro-heterogeneity, and remained to be miscible up to near the cloud points. But they readily phase-decomposed into immiscible blends when heated above the cloud point.

A phase-separated pattern gradually appeared above a specific high temperature (*ca.* 287–320°C). DSC measurements were performed to confirm phase separation above the cloud points. Figure 4 shows the second-scan DSC thermograms for PPO/PαMS blends, which were quenched from temperatures above the cloud point and then scanned in DSC at 20°C min^{-1}. DSC characterization showed two distinct T_gs for the heated/quenched samples, while the original as-cast blends exhibited a single T_g. We thus concluded that blends above the cloud point are composed of nearly pure PαMS phase and a partially mixed PPO/PαMS phase.

Table I. Assignment for ^{13}C chemical shifts of the PPO/PαMS = 50/50 (weight ratio) blend

Peak label	Chemical shift (ppm)	Type of carbon
a	155	C–O (aromatic, PPO)
b	150	aromatic CH (PαMS)
c	145	quaternary carbon (aromatic, PPO)
d	133	C–CH_3 (aromatic, PPO)
e	127	aromatic CH (PαMS)
f	117 112	aromatic CH (PPO)
g	63 57	β-CH_2 (PαMS)
h	45	α-carbon (PαMS)
i	25	methyl (PαMS)
j	16	methyl (PPO)

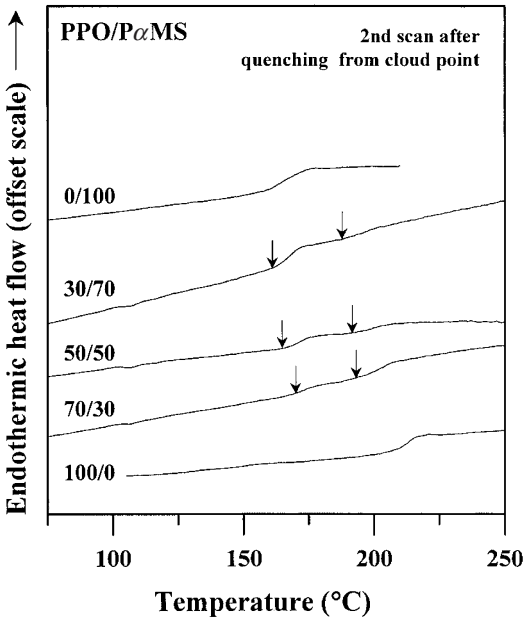

Figure 4. DSC traces of the second scan of PPO/PαMS blends after quenching from above cloud point.

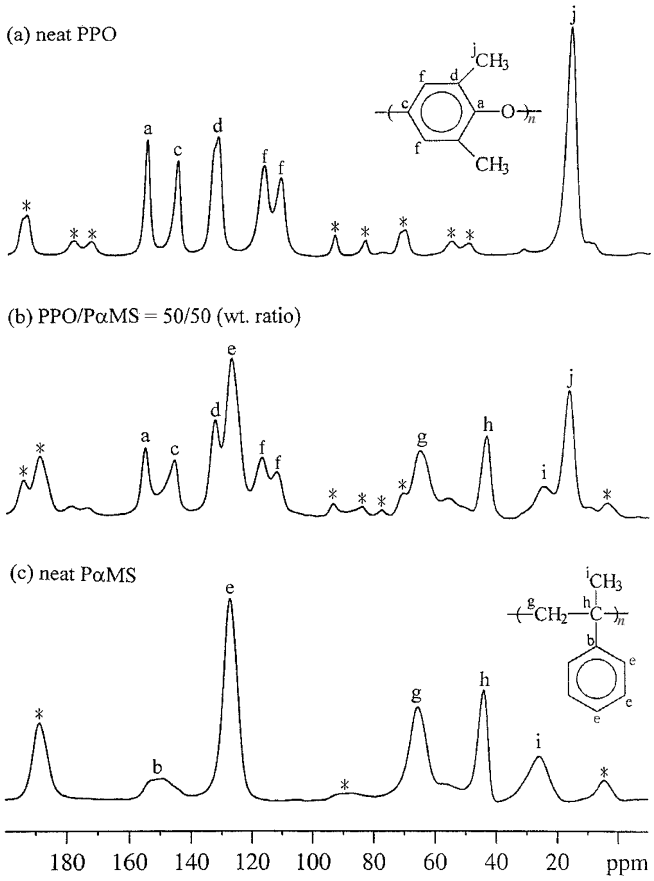

Figure 5. ^{13}C CP/MAS NMR spectra of (a) neat PPO, (b) neat PαMS, and (c) the PPO/PαMS blend (50/50, wt. ratio), examined at room temperature and spinning speed of 6.2 kHz.

^{13}C CP/MAS NMR

^{13}C CP/MAS NMR spectra of neat PPO, neat PαMS and the 50/50 blend at room temperature are shown in Figure 5. In general, the resolution of various polymer carbon signals was quite good. The corresponding resonances were assigned to specified carbons as indicated in the inset structures and are summarized in Table I. The spectrum of neat PPO consists of five resonance lines in the range of 100–160 ppm, which arises from the carbon sites in the aromatic ring, and the resonance at 16 ppm was due to methyl groups. The assignment of the chemical shift in the spectrum of neat PPO is consistent with the previous paper by Bielecki *et al.*[36] In the PαMS spectrum, resonances at 150 and 127 ppm are assigned to non-protonated and protonated aromatic carbons, respectively. Resonances at 63 and 45 ppm were ascribed to the β- and α-carbons, respectively, and the resonance at 25 ppm was assigned to methyl groups. The ^{13}C signal of β-CH_2 in neat PαMS overlaps with the spinning sidebands associated with the resonance at 127 ppm.

A faster spinning speed (13 kHz) was used to acquire the spectrum to avoid interference from spinning side-

Table II. Experimental relaxation time (T_1^H) for neat PPO, neat PαMS, and their blends

PPO/PαMS (wt. ratio)	PPO T_1^H(s)[a]				PαMS T_1^H (s)[a]		
	133 ppm	117 ppm	112 ppm	T_1^H (av)[b]	127 ppm	45 ppm	T_1^H (av)[b]
100/0	0.40	0.36	0.38	0.38	–	–	–
70/30	0.53	0.60	0.64	0.59	0.59	0.60	0.60
50/50	0.69	0.63	0.68	0.66	0.67	0.67	0.67
0/100	–	–	–	–	0.69	0.60	0.65

[a]Accuracy of measurement is ±10%. [b]Average values.

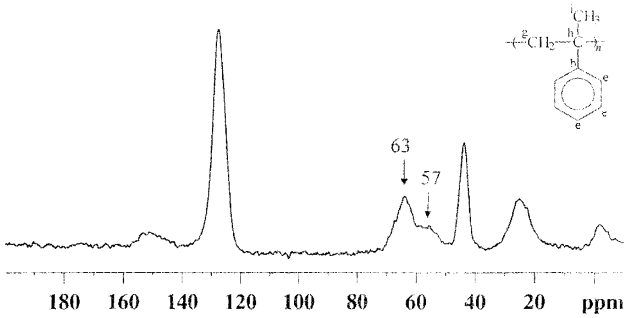

Figure 6. ^{13}C CP/MAS NMR spectra of neat PαMS, examined at room temperature and at high spinning speed of 13 kHz.

bands, and this facilitated assignment of the chemical shift of β-CH_2 in the spectrum of neat PαMS, as shown in Figure 6. Compared to the previous figure, two peaks were resolved at *ca.* 63 and 57 ppm which can be assigned to the mmm and rrr microstructures of PαMS, respectively.[37] Both the α- and β-carbon signals were split, showing part of the PαMS stereo-chemical structure in the solid state.[37] In the spectrum of the 50/50 blend (shown earlier in Figure 5b), the peak of the quaternary carbon in the aromatic ring of PαMS (150 ppm) overlaps with those of PPO (155 and 145 ppm). The spectrum of the blend is merely a superposition of the spectra of pure PPO and PαMS. There was no detectable difference in the chemical shift or line shape between the pure component and blends, and thus the ^{13}C chemical shift does not provide direct information on interactions between PPO and PαMS.

Measurement of T_1^H

By comparing proton relaxation times for the blends with those of pure components, it may be possible under certain circumstances to estimate the upper limit of the length scale of heterogeneity present in blends. If the scale is sufficiently short to permit rapid diffusion of the proton spin energy, a single-component relaxation process will be observed.

In T_1^H experiments, inversion–recovery was used, and the intensities of various carbon resonances of PPO, PαMS, and their blends were measured as a function of delay time τ. Magnetization of resonances $M(\tau)$

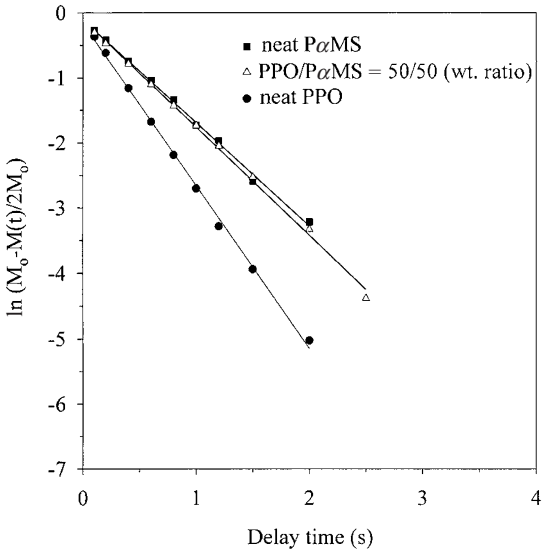

Figure 7. Logarithmic plots of ^{13}C resonance intensity as a function of delay time τ for neat PPO, neat PαMS, and PPO/PαMS blend (50/50, wt. ration) at room temperature. The slope yields T_1^H.

relaxed at single exponential function should obey the following equation:[38]

$$M(\tau) = M_0\left[1 - 2\exp\left(-\tau/T_1^H\right)\right] \quad (1)$$

where M_0 is the intensity of the resonance at $\tau \geq 5\,T_1^H$. Taking the natural logarithm of both sides we obtain,

$$\ln\left[(M_0 - M(\tau))/(2M_0)\right] = -\tau/T_1^H \quad (2)$$

where $\ln[(M_0 - M(\tau))/(2M_0)]$ was plotted versus delay time τ to yield T_1^H.

Figure 7 shows logarithmic plots of the ^{13}C resonance intensities of PPO, PαMS and their 50/50 blend versus delay time τ. The experimental data fit eq 2 quite well in the whole delay time range. Experimental T_1^H relaxation times for the pure components and for blends are given in Table II. Close examination of the experimental T_1^H data shows that the various carbon signals in each pure polymer are characterized by the same T_1^H (*i.e.*, 0.38 and 0.65 s for PPO and PαMS, respectively), within experimental error of 10%. For the 50/50 blend, the signal is best fitted by a single exponential with the T_1^H of 0.66 s within 10% experimental errors, which are nearly the same for various carbons. The observation

Table III. Experimental relaxation time ($T_{1\rho}^H$) for neat PPO, neat PαMS, and their blends

PPO/PαMS (wt. ratio)	PPO $T_{1\rho}^H$(ms)				PαMS $T_{1\rho}^H$ (ms)		
	133 ppm	117 ppm	112 ppm	$T_{1\rho}^H$ (av)[b]	127 ppm	45 ppm	$T_{1\rho}^H$ (av)[b]
100/0	49.1	47.1	47.7	48.5	–	–	–
70/30	20.9	21.0	22.3	21.3	18.9	18.6	18.8
50/50	13.6	15.1	13.6	13.9	13.3	13.6	13.4
0/100	–	–	–	–	7.0	7.0	7.0

[a]Accuracy of measurement is ±10%. [b]Average values.

of a single T_1^H indicates that the domain size of these blends is smaller than the spin-diffusion path length within T_1^H and blends are completely homogeneous on a scale of a few tens of nanometers at the studied compositions.

A useful approximate estimation of the upper limit to the domain size may be estimated by[39–41]

$$\langle L \rangle \cong (6DT)^{1/2} \quad (3)$$

where $\langle L \rangle$ is the average path length for the spin diffusion, D the spin diffusion coefficient, and T the characteristic time (T_1^H or $T_{1\rho}^H$) for spin diffusion, determined by average proton-proton distance and dipolar interaction. Typical D is reported to be $1\sim5 \times 10^{-16}$ $m^2\ s^{-1}$.[39–41] Thus by either T_1^H or $T_{1\rho}^H$ the order of spatial dimensions can be found. D is recently reported to be 8×10^{-16} $m^2\ s^{-1}$ for the PMMA/polystyrene block copolymer.[41] Using this value and = 0.66 s, we obtain the upper limit of $\langle L \rangle \approx$ 20–30 nm for the 50/50 blend.

Measurement of $T_{1\rho}^H$

$T_{1\rho}^H$ can be determined by monitoring the decay of the intensities of resonance lines by varying the spin-lock time (τ). $T_{1\rho}^H$ follows:

$$\ln [M(\tau)/M_0] = -\tau/T_{1\rho}^H \quad (4)$$

where M_0 is the initial equilibrium magnetization, and $T_{1\rho}^H$ can be determined from the slopes of the plots of $\ln [M(\tau)/M_0]$ *vs.* τ. Plots of $T_{1\rho}^H$ decay for the magnetization of the selected carbons in neat PPO, neat PαMS and PPO/ PαMS (50/50) blend are given in Figure 8. The corresponding $T_{1\rho}^H$ are summarized in Table III. $T_{1\rho}^H$ of the carbon resonances for each pure component remain the same within an error of 10%. A spin diffusion process thus occurs sufficiently fast among all protons in both materials. The selected carbons for PPO and PαMS fractions in each blend exhibit single $T_{1\rho}^H$ relaxation behavior, and $T_{1\rho}^H$ can be considered identical within 10% experimental error. Both signals at 63 and 57 ppm for the β-CH_2 groups of PαMS belonging to different microstructures exhibit similar $T_{1\rho}^H$, suggesting that the configuration sequence in PαMS does not play an important role in miscibility with PPO. Since these $T_{1\rho}^H$ are intermediate those of individual blend components, we conclude that the components are mixed at the molecular level at 50/50 composition. Using these observed $T_{1\rho}^H$ relaxation times and taking into account that in the rotating frame the spin diffusion coefficient D is scaled by a factor of 1/2,[41] spin diffusion occurs among all protons in a length-scale range of 20–30 Å in the blends. In other words, PPO and PαMS are mixed in a miscible state and no detectable domains are present on the scale of 20–30 Å or above.

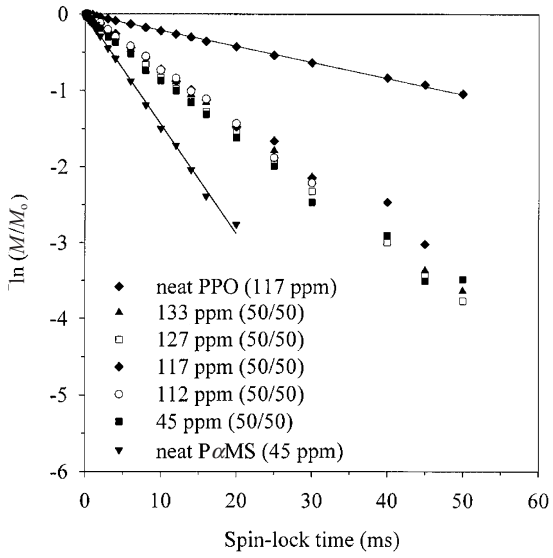

Figure 8. Logarithmic plots of ^{13}C resonance intensity as a function of spin lock time τ for neat PPO, neat PαMS, and PPO/PαMS blend (50/50, wt. ratio) at room temperature. The slope gives $T_{1\rho}^H$.

CONCLUSIONS

Microscopy and DSC showed LCST behavior in the PPO/PαMS blend system. FT-IR revealed no specifically strong intermolecular interactions between the PPO and PαMS polymer chains. Miscibility for the PPO/PαMS blend system is similar to that widely reported for the classically well-known miscible PPO/PS blend system, except that the later (PPO/PS) is miscible showing no LCST (up to experimental temperature

limits of 350 °C or so). By comparison, the present blend system (PαMS/PPO) in this study, though still miscible, exhibited an LCST at ~287 °C, meaning that the originally miscible blend constituents (*i.e.*, PαMS, PPO) may become de-mixed at or above 287 °C.

Thus, to obtain further information, solid-state NMR study was made. We compared the phase behavior of PPO/PαMS blends with that of PPO/PS. The spin-lattice relation time of ^{13}C due to ^{13}C–proton dipole–dipole interaction was then performed to evaluate possible differences in the phase domains and/or phase micro-heterogeneity between the PPO/PαMS and PPO/PS systems. $T_{1\rho}^{H}$ data demonstrated that PPO and PαMS in the blend compositions are molecularly mixed with no detectable domains up to the scale of 20–30 Å. Therefore, T_{1}^{H} and $T_{1\rho}^{H}$ concluded phase homogeneity in the PPO/PαMS blend, which is in good agreement with thermal analysis using DSC. The PPO/PαMS blend system is thus similar to classical PPO and PS blend, in terms of the length scale of homogeneity, expect for LCST behavior in the former.

Acknowledgments. The financial support (NSC 90-2216-E006-030) for this work by the National Science Council of Taiwan is gratefully acknowledged. The many excellent and helpful corrections suggested by the referee(s) have made this paper much better in content and made of presentation and for which the authors express their sincerest thanks.

REFERENCES

1. J. Stoelting, F. E. Karasz, and W. J. MacKnight, *Polym. Eng. Sci.,* **10**, 133 (1970).
2. A. R. Shultz and B. M. Beach, *J. Appl. Polym. Sci.,* **16**, 461 (1972).
3. A. F. Yee, *Polym. Eng. Sci.,* **17**, 213 (1977).
4. S. T. Wellinghoff, J. L. Koenig, and E. J. Baer, *Polym. Sci. USSR*, **15**, 1913 (1977).
5. D. Lefebvre, B. Jasse, and L. Monnerie, *Polymer,* **22**, 1616 (1981).
6. M. B. Djordjevic and R. S. Porter, *Polym. Eng. Sci.,* **23**, 650 (1983).
7. J. Ko, Y. Park, and S. J. Choe, *J. Polym. Sci., Part B: Polym. Phys.,* **36**, 1981 (1998).
8. I. O. Volkov, M. M. Gogelova, A. J. Pertsin, L. V. Filimonova, M. A. P. R. Torres, and C. M. F. Oliveira, *J. Appl. Polym. Sci.,* **68**, 517 (1998).
9. Y. M. Boiko and R. E. Prudhomme, *J. Appl. Polym. Sci.,* **74**, 825 (1999).
10. S. Saeki, J. M. G. Cowie, and I. J. McEwen, *Polymer,* **24**, 60 (1983).
11. J. M. G. Cowie and I. J. McEwen, *Polymer,* **26**, 1667 (1985).
12. J. M. Widmaier and G. Mignard, *Eur. Polym. J.,* **23**, 989 (1987).
13. J. L. Lin and R. J. Roe, *Macromolecules,* **20**, 218 (1987).
14. H. A. Schneider and P. Dilger, *Polym. Bull.,* **21**, 265 (1989).
15. A. Rameau, Y. Gallot, P. Marie, and B. Farnoux, *Polymer,* **30**, 386 (1989).
16. T. A. Callaghan and D. R. Paul, *Macromolecules,* **26**, 2439 (1993).
17. J. R. Fried, T. Lorenz, and A. Ramdas, *Polym. Eng. Sci.,* **25**, 1048 (1985).
18. A. Maconnachie, J. R. Fried, and P. E. Tomlins, *Macromolecules,* **22**, 4606 (1989).
19. L. C. Dickinson, H. Yang, C. W. Chu, R. S. Stein, and J. C. W. Chien, *Macromolecules,* **20**, 1757 (1987).
20. F. Mikes and H. Morawetz, *Macromolecules,* **13**, 969 (1980).
21. J. Kressler, H. W. Kammer, K. Herzog, and H. Heyde, *Acta Polym.* **41**, 1 (1990).
22. E. O. Stejskal, J. Schaefer, M. D. Sefcik, and R. A. McKay, *Macromolecules,* **14**, 275 (1981).
23. L. C. Dickinson, H. Yang, C.-W. Chu, R. S. Stein, and J. C. Chien, *Macromolecules,* **20**, 1757 (1987).
24. T. Yu and M. Guo, *Prog. Polym. Sci.,* **15**, 825 (1990).
25. E. O. Stejskal, J. Schaefer, M. D. Sefcik, and R. A. McKay, *Macromolecules,* **14**, 275 (1981).
26. M. Guo, *Trends Polym. Sci.,* **4**, 238 (1996).
27. R. H. Lin, E. M. Woo, and J. C. Chiang, *Polymer,* **42**, 4289 (2001).
28. R. R. Wu, H. M. Kao, J. C. Chiang, and E. M. Woo, *Polymer,* **43**, 171 (2002).
29. A. Asano, K. Takegoshi, and K. Hikichi, *Polymer,* **35,** 5630 (1994).
30. S.-Y. Kwak and N. Nakajima, *Macromolecules,* **29**, 3521 (1996).
31. S.-Y. Kwak and N. Nakajima, *Macromolecules,* **29**, 5446 (1996).
32. N. Parizel, F. Laupretre, and L. Monnerie, *Polymer,* **38**, 3719 (1997).
33. K. S. Jack and A. K. Whittaker, *Macromolecules,* **30**, 3560 (1997).
34. J. White and D. J. Lohse, *Macromolecules,* **32**, 958 (1999).
35. M. Gordon and J. S. Taylor, *J. Appl. Chem.,* **2**, 493 (1952).
36. A. Bielecki, D. P. Burum, D. M. Rich, and F. E. Karasz, *Macromolecules,* **24**, 4820 (1991).
37. R. F. Nogueira and M. I. B. Tavares, *Polym. Test*, **20**, 379 (2001).
38. H. Friebolin, "Basic One- and Two-Dimensional NMR Spectroscopy", VCH Publishers, New York, N.Y., 1991, chapt. 7, Relaxation, p 162.
39. V. J. McBriety, D. C. Douglass, and T. K. Kwei, *Macromolecules,* **11**, 1265 (1978).
40. D. E. Demco, A. Johansson, and J. Tegenfeldt, *Solid State Nucl. Magn. Reson.*, **4**, 13 (1995).
41. J. Clauss, K. Schmidt-Rohr, and H. W. Spiess, *Acta Polym.*, **44**, 1 (1993).